INL/CON-18-51659-Revision-0

Thermal Model Details and Description of the AGR-5/6/7 Experiment

Grant L Hawkes

May 2019

The INL is a U.S. Department of Energy National Laboratory
operated by Battelle Energy Alliance

INL/CON-18-51659-Revision-0

Thermal Model Details and Description of the AGR-5/6/7 Experiment

Grant L Hawkes

May 2019

Idaho National Laboratory
Idaho Falls, Idaho 83415

http://www.inl.gov

Prepared for the
U.S. Department of Energy

Under DOE Idaho Operations Office
Contract DE-AC07-05ID14517

ICAPP 2019 – International Congress on Advances in Nuclear Power Plants
France, Juan-les-pins – 2019, May 12 | 15

Thermal Model Details and Description of the AGR-5/6/7 Experiment

Grant Hawkes[1*], James Sterbentz[1], Mitchell Plummer[1]

[1]Idaho National Laboratory, 2525 Fremont, MS 3870, Idaho Falls, Idaho, USA
[*]Corresponding Author, E-mail: Grant.Hawkes@inl.gov

The AGR-5/6/7 experiment is currently being irradiated in the Advanced Test Reactor (ATR) at the Idaho National Laboratory and is approximately 25% complete. Several fuel and material irradiation experiments have been planned for the U.S. Department of Energy Advanced Gas Reactor Fuel Development and Qualification Program, which supports the development and qualification of tristructural isotropic (TRISO) coated particle fuel for use in high-temperature gas-cooled reactors. The goals of these experiments are to provide irradiation performance data to support fuel process development, qualify fuel for normal operating conditions, support development of fuel performance models and codes, and provide irradiated fuel and materials for post-irradiation examination and safety testing. Originally planned and named as separate fuel experiments, but subsequently combined into a single test train, AGR-5/6/7 will test low-enriched uranium oxycarbide (UCO – a heterogeneous mixture of uranium oxide and uranium carbide) TRISO fuel. The AGR-5/6 portion of the experiment will provide data to support qualification of the selected reference fuel design, while the AGR-7 portion will serve as a margin test, irradiating the fuel beyond normal operating conditions. A thermal finite element model detailing gas gaps, thermal conductivity varying with temperature and fast neutron fluence, radiation heat transfer, and graphite shrinkage is presented herein.

KEYWORDS: AGR-5/6/7, TRISO Fuel, Thermal Model

Introduction

Irradiation experiments of tristructural isotropic (TRISO) particle fuel are being conducted to support development of the next generation high temperature gas reactors in the United States. The Advanced Gas Reactor (AGR) Fuel Development and Qualification Program, which is part of the Advanced Reactor Technologies (ART) Program, is responsible for these experiments, which demonstrate and qualify new low enriched uranium (LEU) TRISO particle fuel for use in high temperature gas cooled reactors. The goals of the irradiation experiments are to provide irradiation performance data to support fuel process development, to qualify fuel for normal operating conditions, to support development and validation of fuel performance models, and to provide irradiated fuel and materials for post irradiation examination (PIE) and safety testing. The experiments each consist of multiple separate capsules, and are irradiated in an inert sweep gas atmosphere with individual on line temperature monitoring and control of each capsule. The sweep gas also has on line fission product monitoring of its effluent to track performance of the fuel in each individual capsule during irradiation.

Originally seven separate experiments were envisioned to meet various program objectives. The last three tests are being combined into a single irradiation (AGR 5/6/7). These tests serve as the formal fuel qualification irradiations (AGR 5/6) and the margin test (AGR 7). The purpose of the margin test is to demonstrate that there is a margin between the highest fuel temperature in an operating high temperature gas reactor (HTGR) and the temperature at which fuel particle failure rate becomes unacceptable.

The AGR 5/6/7 experiment will be irradiated at the Idaho National Laboratory (INL) in the Advanced Test Reactor (ATR) northeast flux trap irradiation position. The experiment will consist of a number of individual capsules each equipped with its own temperature control system and fission product gas monitoring capability. The different capsules will experience a range of temperatures, fuel burnup, and fast fluence to envelope the range of operational conditions in a future HTGR reactor.

A thermal finite element model has been created for the five capsules comprising the AGR-5/6/7 experiment. Previous thermal models (1), (2), (3) of AGR experiments have been successful in the past. The experiment is composed of five separate stainless steel capsules all welded together. There are a total of 194 fuel compacts with 170 in the AGR-5/6 portion and 24 in the AGR-7 portion. Heat rates and fast neutron fluence were input from a detailed physics analysis using the Monte Carlo N-Particle (MCNP) code. Individual heat rates for each non-fuel component were input as well. ATR outer shim control cylinders and neck shim rods along with ATR driver fuel power and fuel depletion were incorporated into the physics heat rate calculations. Surface-to-surface radiation heat transfer along with conduction heat transfer through the gas mixture of helium-neon (used for temperature control) was used in the thermal calculations. Each capsule has its own helium-neon mixture. Graphite shrinkage due to the fast neutron fluence is incorporated into the model. Gas gaps change as a function of fast neutron fluence. This is a large model with more than 1 million finite element brick elements. More than 150 different parts are modeled in the finite element model and communicate with each other from a heat transfer sense. More than 50 thermocouples are used in the experiment and are compared to actual measurements.

Model Description

The AGR-5/6/7 experiment is placed in the northeast flux trap of the ATR as shown in Figure 1. The experiment is comprised of five individual capsules all welded together in a vertical orientation as shown in Figure 2 (top at left, water flowing down). The outside diameter of the stainless steel capsules is 0.070231 m, with a total experiment length of approximately 1.2192 m. Each capsule contains TRISO compacts that are nominally 0.0127 m. in diameter with a length of 0.0254 m. Capsules 1 and 5 have a TRISO fuel particle packing fraction of 40%, while capsules 2-4 have a packing fraction of 25%. The particles are bound together by a carbon matrix material.

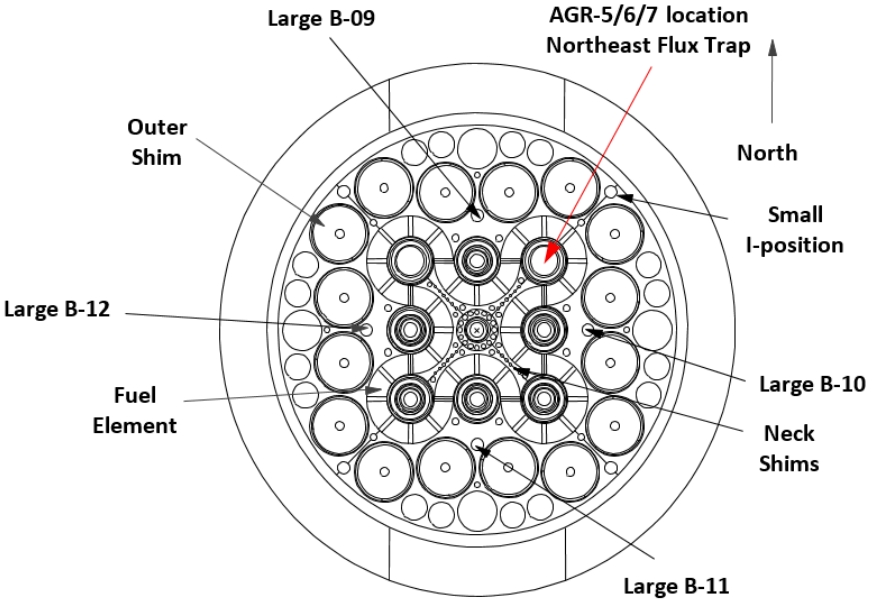

Figure 1. ATR core cross section showing the northeast flux trap position containing the AGR-5/6/7 experiment.

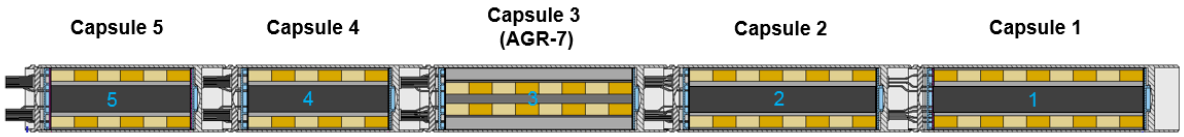

Figure 2. Capsule layout diagram (capsule 5 on top, vertical experiment).

Coolant water flows downward on the outside of the capsules at approximately 12.0 m/s and enters the experiment at 51°C. Program goals for power density, packing fraction, temperature, fluence, and burnup are shown in Figure 3. These program goals are compared to past German and Japanese TRISO experiments. The various layers of the TRISO fuel particle are displayed in Figure 4. Capsule cross section views are displayed in Figure 5. Capsule 1 has 10 stacks, while capsules 2, 4, and 5 have four stacks, capsule 3 has three stacks arranged in an inner graphite holder to raise the temperature. Thru tubes are located in capsules 2-5 to hold the thermocouple wires and gas lines.

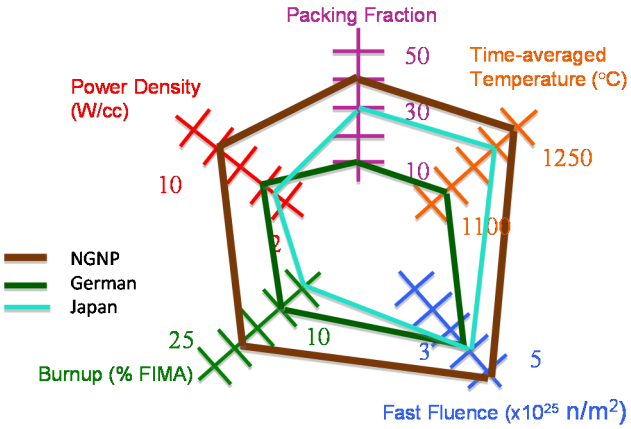

Figure 3. Program goals for power density, packing fraction, temperature, fluence, and burnup.

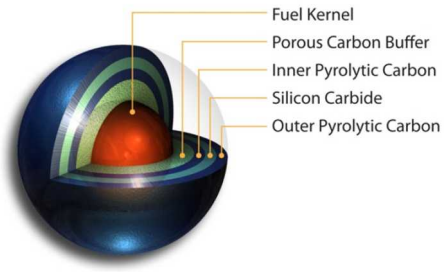

Figure 4. TRISO fuel partcle description and layout.

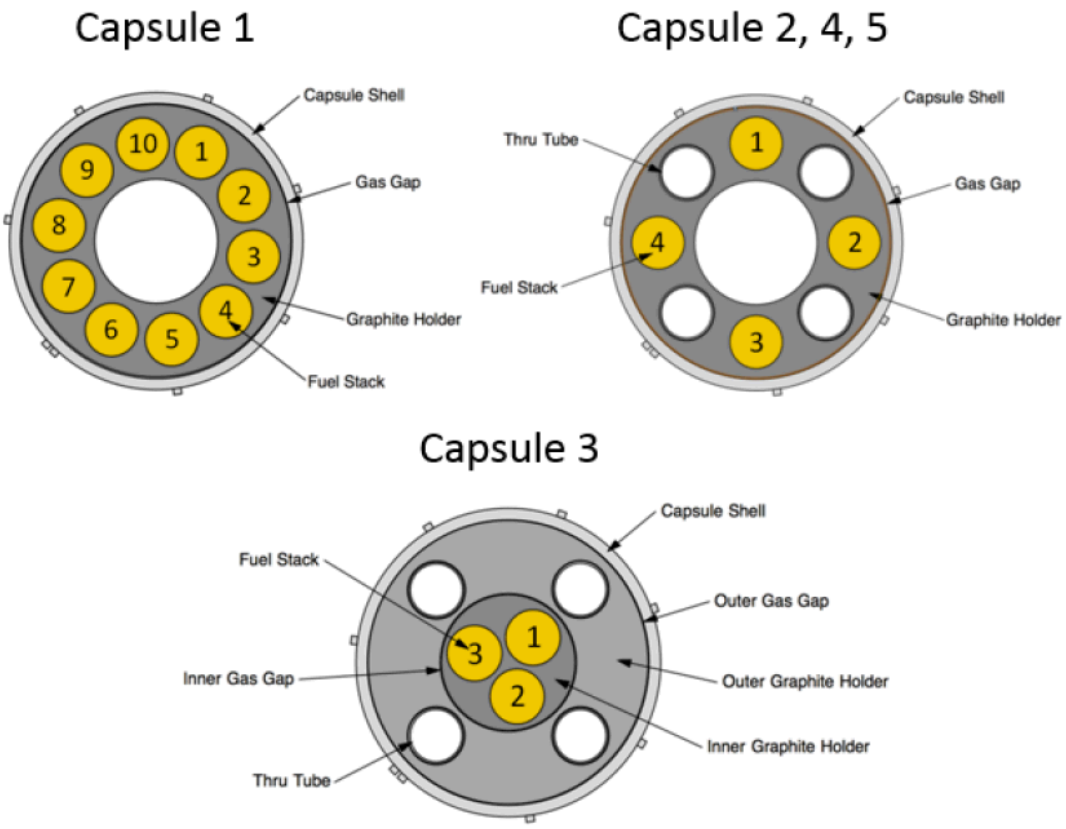

Figure 5. Capsule cross sectional view for the five capsules.

A summary of the capsule particles, fuel target temperatures, and gas gap between the graphite holder and stainless steel capsule wall are shown in Table 1. Approximately 54% of the particles are in

capsule1. Hot gas gaps are listed in the last column. These hot gas gaps were designed to shape the temperature profile of the compacts. Three different methods are available to control the temperature in each capsule: (1), adjust the helium/neon gas mix, (2) adjust the northeast lobe power, and (3) change the neutron filter on the outside of the experiment. Each ATR cycle is approximately 55 days. The neutron filter can only be changed during the shutdown time between cycles.

Capsule Summary					
	Length (m)	Number of Compacts	Number of Particles	Target Temperature Range (°C)	Hot gas gap top half / Hot gas gap bottom half (mm)
Capsule 5	0.1524	24	82,608	<900	0.3302 / 0.2032
Capsule 4	0.1524	24	54,600	900 – 1050	0.2540 / 0.2032
Capsule 3	0.2032	24	54,600	1350 – 1500	0.2032 / 0.1524 / 0.2032
Capsule 2	0.2032	32	72,800	900 – 1050	0.1778 / 0.2032
Capsule 1	0.2286	90	309,780	900 - 1350	0.1524 / 0.2032
Totals	0.9398	194	574,388		

Table 1. Capsule summary for length, compacts, particles, target temperature range, and hot gas gaps.

The finite element heat transfer code ABAQUS (4) was used to model the experiment. Figure 6 shows the cut-away view of the finite element mesh of the entire capsule train. There are approximately 1,200,000 hexahedral finite element bricks in the model. Figure 7 shows the finite element mesh of capsule 1. The figure shows the thermocouples and gas lines protruding out of the top. There are no thru tubes in this capsule. There are 10 stacks of fuel. These capsules are designed to transfer heat in the radial direction as zirconia insulators and gaps are placed on top and bottom of the capsule to insulate it in the axial direction. The top of capsule 1 is an exception as a ring spring on the bottom pushes up on the graphite holder and fuel and making good contact with the top. This was done since there is a lot of heat generation at the top of the fuel and it can conduct out through the top stainless steel cap and into the coolant water. The top and bottom caps of all the capsules are tapered in order to remove material and hence gamma heat. There are very small gas gaps between the thermocouple and its sheath and between the sheath and the graphite holder. Figure 8 shows the finite element mesh of capsule 2 and represents capsules 4 and 5 also since they are similar. The thru tubes (made out of stainless steel) and thru tube protective sleeves (molybdenum) along with thermocouples and gas lines are protruding out the top of the top cap. Gamma heat produced from the gas lines and thermocouples that go through the thru tubes is modeled as a surface heat flux on the inside of the thru tubes.

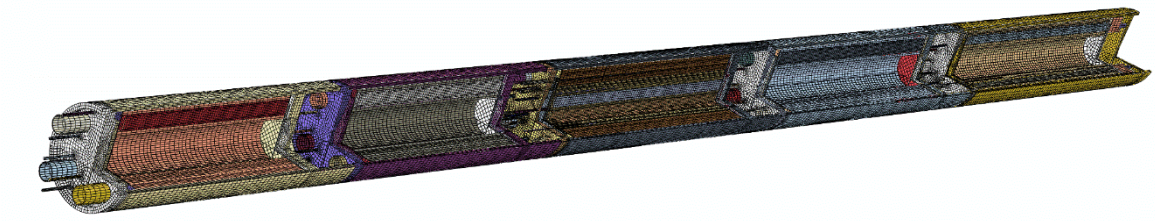

Figure 6. Cut-away view of finite element mesh of entire capsule train.

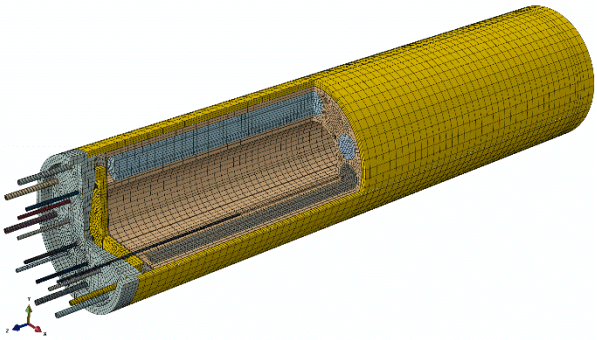

Figure 7. Cut-away view of finite element mesh of capsule 1.

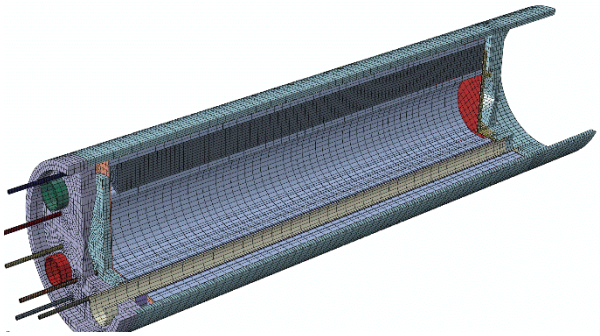

Figure 8. Cut-away view of finite element mesh of capsule 2.

Shown in Figure 9 is a cut-away view of the inside and outside graphite holders and fuel stacks of capsule 3. As noted in Table 1, there are three different outside diameters of the outside holder in order to obtain the temperature distribution necessary. The fuel stacks are all inside the inside graphite holder and run at very high temperatures as noted in Table 1. Figure 10 shows a cut-away view of the finite element mesh of capsule 3 with the thru tubes, thru tube liners, and thermocouples protruding out of the top. A plenum area between the capsules allows for the bending of the thermocouples and gas lines from the thru tubes above and into their individual holes for the capsule below. This plenum is very cool since there is only a small amount of gamma heat being produced and coolant water running along the outside of the capsule wall. The thermocouples and thru tubes were modeled as protruding upwards approximately 25.4 mm and radiate and conduct to the cooler plenum walls. Perfect contact is assumed between the thermocouples and capsule top cap. Same also for the thru tube protective sleeves and top cap.

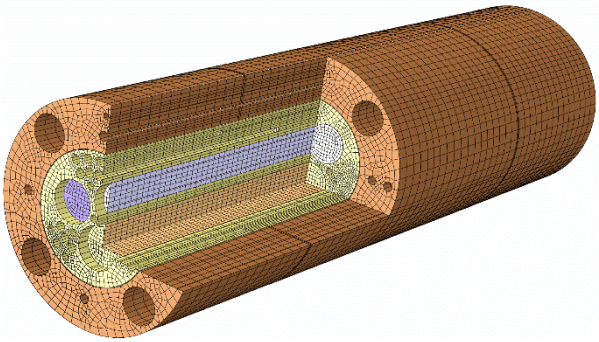

Figure 9. Cut-away view of finite element mesh of inner and outer graphite holder for capsule 3.

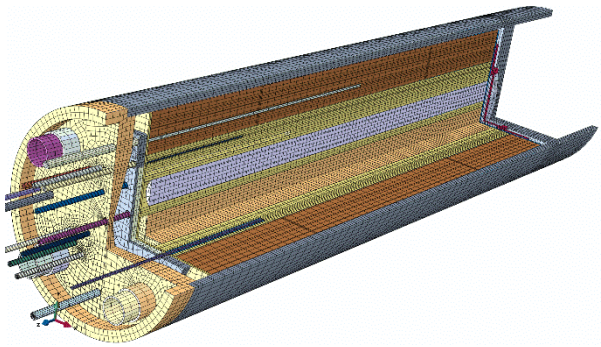

Figure 10. Cut-away view of finite element mesh of capsule 3.

Fuel Compacts

The fuel compacts are modeled as having a thermal conductivity described in great detail in Reference (1). The packing fraction and matrix density for capsules 1 and 5 are 40% and 1.73 g/cm^3, while capsules 2-4 are 25% and 1.75 g/cm^3. The compacts are taken as perfect contact with the bottom graphitic material. The gaps between the compacts and holder are calculated from as-built dimensions. Each compact was measured and compared to each hole in each graphite holder. The exact as-built dimensions were implemented for every stack top half, and bottom half. Heat is transferred via gap conductance and gap radiation. Gap radiation between the compacts and graphite holder was implemented with both surfaces having an emissivity of 0.9.

Graphite Holders

The graphite holders are made out of IG-430 nuclear grade graphite. Experiments conducted on graphite specimens at the INL (5) were used to obtain material properties such as unirradiated and irradiated thermal diffusivity, and graphite shrinkage due to fast neutron fluence. Specific heat values were taken from (6) and implemented in the following equation with temperature in Kelvin.

$$c_p = \frac{1}{11.07 \cdot T^{-1.644} + 0.0003688 \cdot T^{0.02191}} \left(\frac{J}{kg \cdot K}\right) \quad (1)$$

Density was calculated from the following set of equations taking into account the expansion of graphite with temperature:

$$\Delta L = \alpha L(T - T_0), \quad \rho(T) = \rho_0 \frac{V_0}{V(T)}, \quad V_0 = L_0^3, \quad V(T) = (L_0 + \Delta L)^3$$

$$\rho(T) = \frac{\rho_0}{[1 + \alpha(T - T_0)]^3} \quad (2)$$

T_0 was taken as 20°C. Values of ρ_0 (1.815 g/cm^3) and α_0 (5.5e-6 1/°C) were taken from (7) and (8) respectively. To account for change of conductivity due to neutron damage, a conductivity multiplier (9) taken from JAEA was implemented comparing irradiated graphite to unirradiated graphite at each temperature. To convert the Japanese multiplier data (9) from dpa to fast neutron fluence a conversion multiplier of 0.763*fluence=dpa (fluence units scaled by 1x10^{25}) was implemented and is specific to the northeast flux trap of ATR. The fluence energy band is E>0.18MeV and units of 1x10^{25} n/m^2. To convert from the Japanese data of E>0.10MeV, a multiplier of 0.9 * E>0.10MeV = E>0.18MeV. The multiplier and dpa to fluence conversion come from (10). Unirradiated thermal diffusivity data for IG-430 taken from (5) is shown in Figure 11. Values were extrapolated to higher temperatures. Unirradiated thermal conductivity varying with temperature was obtained by multiplying the diffusivity by the specific heat from Eq 1, and the density from Eq 2. Figure 12 shows a graph of the conductivity multiplier (9) varying with temperature and fast neutron fluence. The curve fit developed for this data is shown in Eq 3.

$$\frac{k_{irr}}{k_0} = (p_1 + p_2 \cdot T) + [1 - (p_1 + p_2 \cdot T)] \cdot exp\left(\frac{-F \cdot T}{p_3 + p_4 \cdot T + p_5 \cdot T^2}\right)$$

p_1 = 3.100e-02, p_2 = 5.613e-04, p_3 = 1.29077e+02, p_4 = -9.310e-01, p_5 = 1.826e-03 (3)

where T is temperature in °C and F is fast neutron fluence (x10^{25} n/m^2, E>0.18 MeV). Parameters $p1$ through $p5$ are listed in the equation.

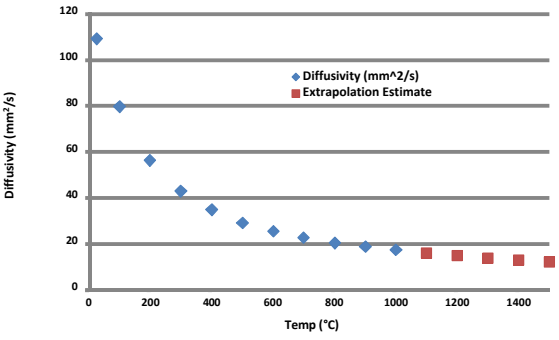

Figure 11. Unirradiated IG-430 thermal diffusivity (mm/s) varying with temperature (°C) (5).

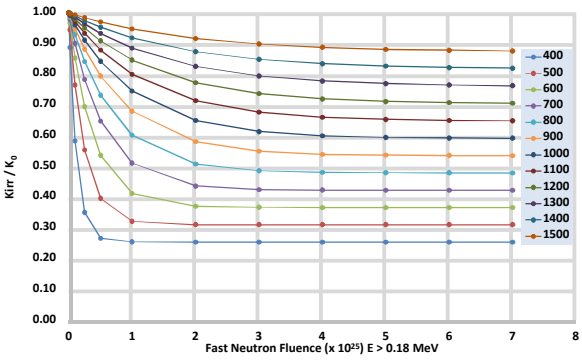

Figure 12. Conductivity multiplier (k_{irr}/k_0) varying with temperature (°C) and fast neutron fluence (9).

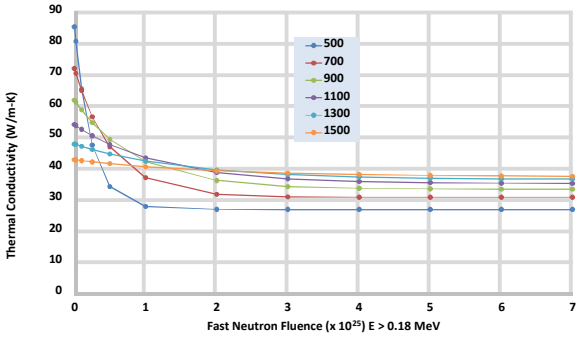

Figure 13 shows the thermal conductivity of IG-430

varying with temperature and fast neutron fluence incorporating the multiplier discussed above. Note a very fast drop off in conductivity for low temperature with a small amount of fast neutron fluence. Almost no change above a fluence value of 3 as the graphite appears to anneal itself and stay in a steady mode. Figure 14 shows a graph of the coefficient of thermal expansion multiplier (9) varying with temperature and fast neutron fluence. The curve fit developed for this data is shown in Eq (4).

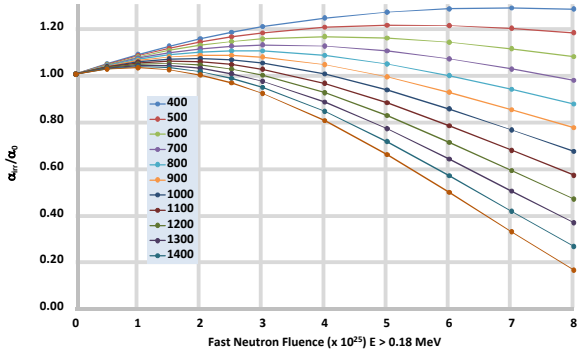

$$\frac{\alpha_{irr}}{\alpha_0} = 1 + (p_1 + p_2 \cdot T) \cdot F + p_3 \cdot T \cdot F^2 + (p_4 + p_5 \cdot T) \cdot F^3$$

p_1 = 1.050e-01, p_2 = -2.974e-05, p_3 = -2.298e-05, p_4 = -3.007e-04, p_5 = 1.350e-06 (4)

where T is temperature in °C and F is fast neutron fluence (x10^{25} n/m^2, E>0.18 MeV). Parameters $p1$ through $p5$ are listed in the equation.

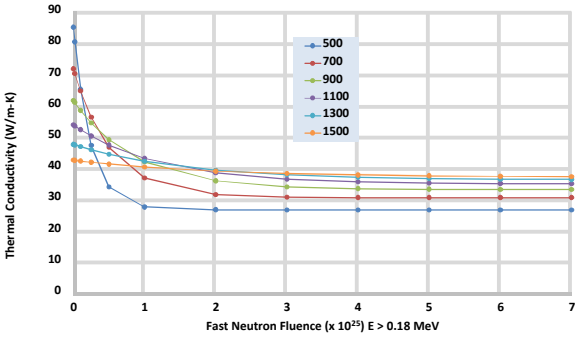

Figure 13. Thermal conductivity of IG-430 varying with temperature (°C) and fast neutron fluence.

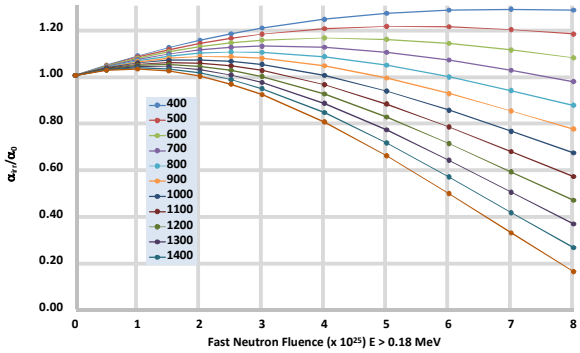

Figure 14. Coefficient of thermal expansion multiplier (α_{irr}/α_0) varying with temperature (°C) and fast neutron fluence (9).

Outer Gas Gaps

The graphite holders undergo neutron damage as irradiation progresses. The graphite also shrinks until a turnaround point and then starts to swell. For this AGR-5/6/7 experiment, this turnaround point is not reached. Diameter change of specimens for IG-430 was taken from (11) and shown in Figure 15. This graphic shows that the outer diameter shrinks (orange), while the inner diameter grows (blue). The slope is shown from linear curve fit to be -0.00146 $\Delta D/D$ per unit of fluence. Thermal conductivity of helium-neon gas mixture was taken

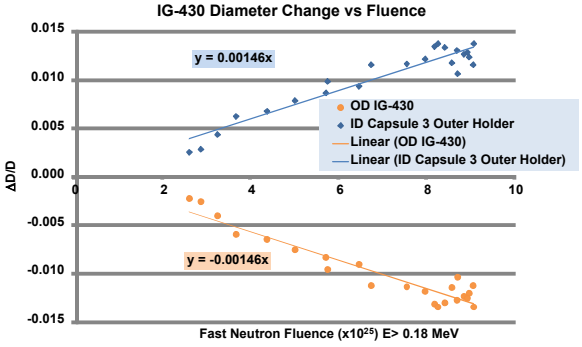

from (12) and shown in 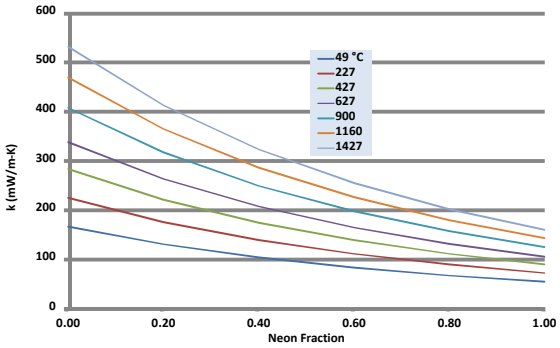

Figure 16.

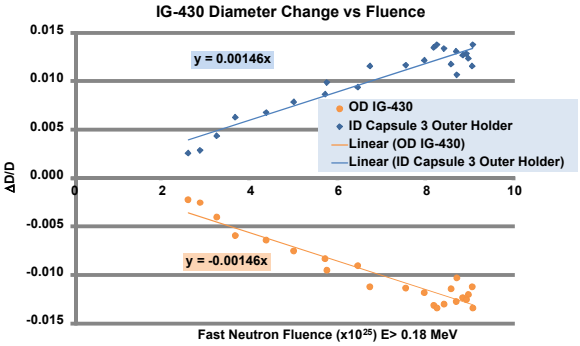

Figure 15. Diameter change of IG-430 varying with fast neutron fluence 11).

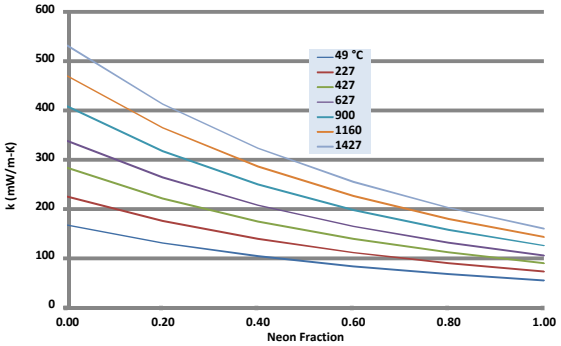

Figure 16. Thermal conductivity (mW/m-K) of helium-neon gas mixture varying with temperature (°C) (12).

The gap conductance user subroutine was used to calculate the heat transfer across the gap on the outside of the graphite holders and the stainless steel capsule wall. The surface temperature of the holder and capsule are made available to the subroutine. Eq. (5) shows the details of the gap conductance across this gap.

$$gap = \left[r_0[\alpha(T_i - T_0) + 1]\right],ss \; - \left[r_0\left[1 + \frac{\Delta r \cdot F}{r} + \alpha(F,T)(T_i - T_0)\right]\right],holder$$

$$gap\ conductance = \frac{kgas(T)}{gap} \quad where\ T = \frac{Ti,ss + Ti,holder}{2}$$

$$where\ T_{i,holder} = \frac{T_{inside,holder} + T_{outside,holder}}{2}$$

$$where\ i = instantaneous,\ \ 0 = original\ at\ room\ temperature \tag{5}$$

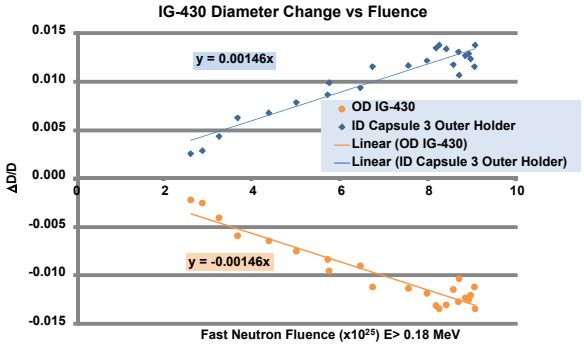

where $\Delta r/r$ is the slope from Figure 15, $kgas(T)$ is the gas mixture thermal conductivity and $\alpha(F,T)$ is described above. Average temperature between the inner and outer surface of the graphite holder is used. Since the inside surface temperature is not available in the subroutine, a vector of the inside surface temperature was obtained from the volumetric heat subroutine and passed into the gap conductance subroutine. Eq 6 shows the gap conductance between the inner and outer graphite holders for capsule 3.

$$gap\ inner3 = \left[r_0\left[1+\frac{\Delta r}{r}+\alpha(F,T)(T_i-T_0)\right]\right]_{,outer} - \left[r_0\left[1+\frac{\Delta r\cdot F}{r}+\alpha(F,T)(T_i-T_0)\right]\right]_{,inner}$$
$$gap\ conductance = \frac{kgas(T)}{gap\ inner3} \quad where\ T=\frac{Ti,inner+Ti,outer}{2} \tag{6}$$

Offset Holder Calculations

The graphite holders are held off of the capsule wall by small nubs of graphite every 90°. The possibility exists for these nubs to wear down with the vibration in the reactor. There is also a slight bit of clearance between the outside of the nubs and the capsule wall. These nubs are left on the holder while still machining the outside diameter to the dimension needed for the gas gap. An offset calculation where the gas gap varies azimuthally is described below. It is possible to move the holder and contents inside the capsule with the ABAQUS CAE model, it is not prudent to do so since one doesn't know which direction the holder might offset. This offset model is included in the gap conductance subroutine and is taken as the r_0 value of the holder. An offset in +/- x and +/-y is available for each capsule individually. After the experiment is irradiated, several runs will be made to see which direction and how much offset needs to be performed for each capsule. These offset values are in the range of 0.03 mm. Figure 17 shows a diagram of the outside (capsule) offset h units in the x direction and k units in the y direction from the graphite holder. Eq. (7) shows the calculations to obtain the x_o, and y_o values since x_i and y_i are given in the subroutine. Even though the finite element mesh model shows the capsule perfectly centered, this new gap is used for the gap conduction equations.

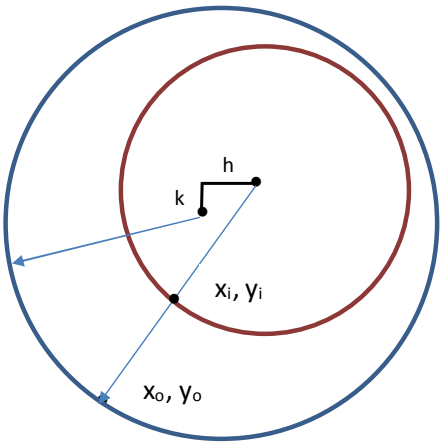

Figure 17. Diagram to calculate gap with capsule wall offset h in x direction and k in y direction.

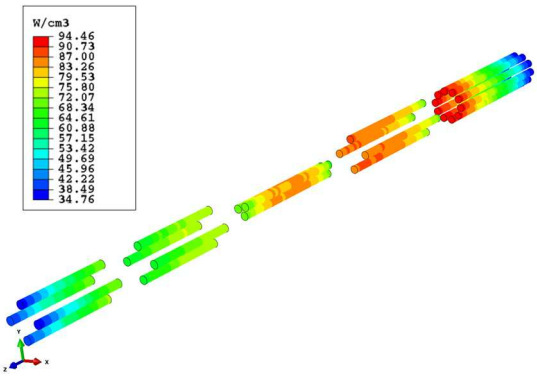

Figure 18. Compact heat generation rates (W/cm^3) imported from physics calculations.

$$a = \left(\frac{y_i}{x_i}\right)^2 + 1, \quad b = -2\cdot\left(\frac{y_i}{x_i}\right)\cdot k - 2\cdot h, \quad c = k^2 + h^2 - r_o^2$$
$$x_o = \frac{-b \pm \sqrt{b^2-4ac}}{2a}, \qquad y_o = \pm\sqrt{r_o^2 - (x-h)^2} + k$$
$$gap = \sqrt{(x_o - x_i)^2 + (y_o - y_i)^2} \tag{7}$$

Heat Rates

Heat rates are taken from results generated from the MCNP code (13) specific to the AGR-5/6/7 experiment. Heat rates are calculated and imported into the ABAQUS input file for each compact (fission), and each 25.4 mm of the height of the graphite holders (gamma). Gamma heat rates are also implemented from the water, stainless steel capsules, thru tubes, thermocouples, and all of the various components on the top and bottom of each capsule.

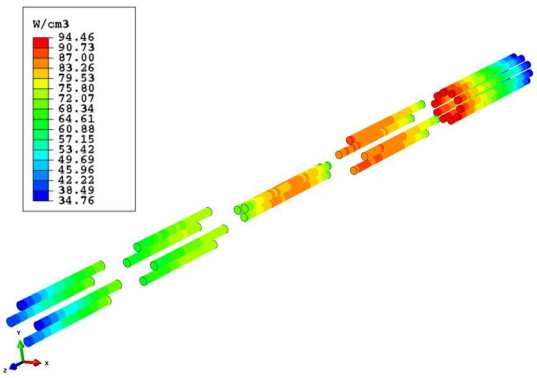

Figure 18 shows volumetric heat generation rates of all of the compacts imported from the physics calculations (top at left). Highest heat rates are at the top of capsule 1 as there is a lot of fissionable material closer to the core center. The gamma heat rates for the graphite holders are in a typical chopped cosine profile.

Results

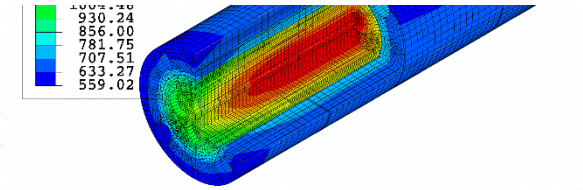

Figure a typical day cut-away view of the entire model with ule 3 and capsule 1 are the hottest. Capsule 3 has a strong temperature gradient in the axial direction, atures ranging in the 700 to 900°C range. Figure 20 shows a cut-away view of the graphite holder and fuel compacts for capsule 3. A large temperature drop across the gap between the inner and outer holder is noticed. Figure 21 shows a history plot for the first 21 days of the measured minus calculated temperatures (°C) of the thermocouples. The first 12 days were run on helium so as to make sure everything was running properly before going up to the desired temperature and mixing in more neon. Capsule 5 shows excellent agreement between the measured and calculated TC temperatures. Capsules 4, 3, and 2 show good agreement with the average difference being about 40 °C. Capsule 1 has a large variation in predictions compared to actual TCs. The average difference looks to be about 60°C while running cool for the first 12 days and around 70°C when running hotter on days 13-20. All of the TC wires for capsule 1 go through the thru tubes of all of the upper four capsules and so these wires see some very high temperatures. The model agrees modestly well with the measured TCs.

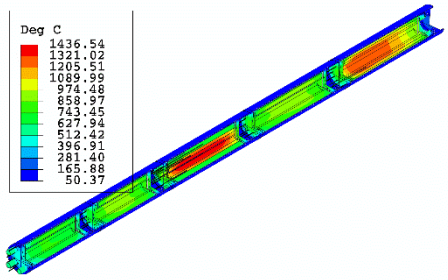

Figure 19. Temperature (°C) contours of cut-away view of entire experiment.

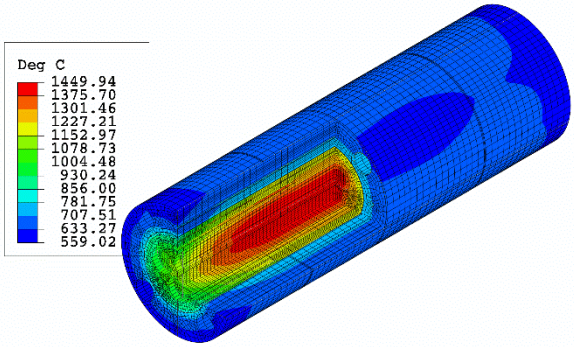

Figure 20. Temperature contours (°C) of cut-away view of capsule 3 graphite holder and fuel compacts.

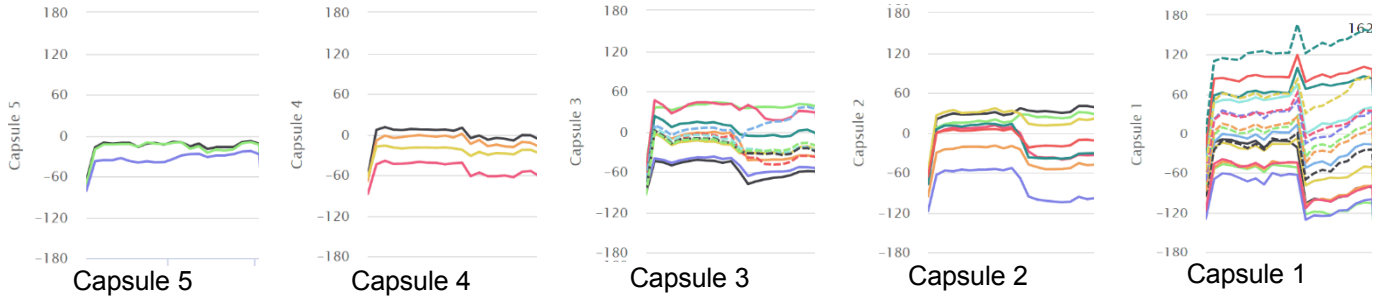

Figure 21. Temperature (°C) difference of measured minus calculated thermocouples for the first 21 days (x axis) for all five capsules.

Figure 22 shows the ten ypical day. The TCs vary in depth and location. The , yet still degrade with temperature and neutrons. Figure 23 shows a straight on top down view of capsule 1 axial mid-plane temperature contours for nominal (left) and the capsule being offset by 0.0254 mm in a southwest direction (right). Since the reactor core center is located southwest of this experiment, the heat rates are slightly higher on the southwest corner of the experiment and hence higher temperatures a shown on the left contour plot. Since the capsule is moved southwest, it makes a larger gap and high temperatures on the southwest side as shown on the right temperature contour plot.

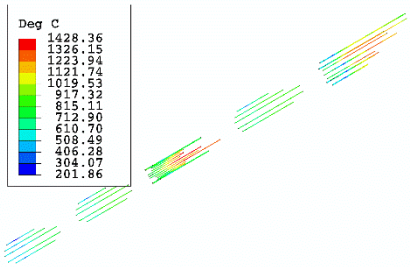

Figure 22. Temperature (°C) contours of thermocouples from all five capsules.

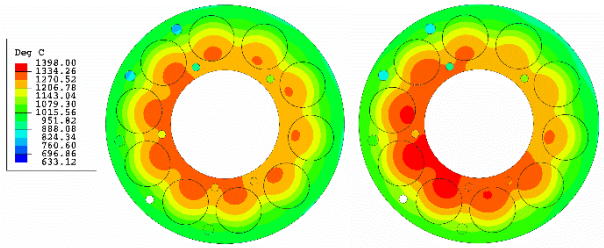

Figure 23. Straight on top down view temperature contours (°C) of capsule 1 graphite holder and fuel compacts at axial mid-plane. Left is capsule centered, right is capsule offset 0.0254 mm in southwest direction.

Conclusion

A thermal finite element model of the AGR-5/6/7 experiment has been created with the ABAQUS software and discussed. Fuel compacts and graphite holder properties vary with temperature and fast neutron fluence. Gas gaps varying because of graphite shrinkage and thermal expansion were discussed. Heat rates for fissionable TRISO fuel compacts and gamma heat rates for all other materials were calculated from the MCNP code and imported into the thermal model. Temperature contours for typical days were shown. Measured minus calculated thermocouple temperatures compare favorably. Results of a capsule being offset from the holder was discussed and displayed.

Acknowledgment Work supported by the U.S. Department of Energy, NGNP Program, Idaho Operations Office Contract DE AC07 05ID14517.

References

1) G. L. Hawkes, J. W. Sterbentz, J. T. Maki, B. T. Pham, “Thermal Predictions of the AGR-3/4 Experiment with Post Irradiation Examination Measured Time-Varying Gas Gaps,” ASME J of Nuclear Rad Sci 3(4), 041007 (Jul 31, 2017), Paper No: NERS-17-1008; doi: 10.1115/1.4037095
2) G. L. Hawkes, J. W. Sterbentz, B. T. Pham, “Thermal Predictions of the AGR-2 Experiment with Variable Gas Gaps,” Nuclear Technology / Volume 190 / Number 3 / June 2015 / Pages 245-253, Technical Paper / Thermal Hydraulics / dx.doi.org/10.13182/NT14-73
3) G. L. Hawkes, J.W. Sterbentz, J. Maki, B. Pham, “Daily Thermal Predictions of the AGR-1 Experiment with Gas Gaps Varying with Time,” paper # 12111, International Congress on the Advances in Nuclear Pow-

er Plants (ICAPP 2012), Chicago, IL, Jun 24-28, 2012.
4) Dassault Systèmes, ABAQUS version 6.14-2, www.simulia.com or www.abaqus.com, Providence, Rhode Island, 2014.
5) William Windes, W. David Swank, David Rohrbaugh, and Joseph Lord. AGC-2 Graphite Preirradiation Data Analysis Report. United States: N. p., 2013. Web. doi:10.2172/1097190.
6) ASTM, 2014. Standard practice for testing graphite and boronated graphite materials for high-temperature gas-cooled nuclear reactor components. Designation C781-08, ASTM International, West Conshohocken, Pennsylvania.
7) Rohrbaugh, David Thomas. AGC 2 Irradiated Material Properties Analysis. United States: N. p., 2017. Web. doi:10.2172/1369362.
8) David Swank, Joseph Lord, David Rohrbaugh, and William Windes. AGC-2 Graphite Pre-irradiation Data Package. United States: N. p., 2010. Web. doi:10.2172/991897.
9) Taiju Shibata, Motokuni Eto, Eiji Kunimoto, Shusaku Shiozawa, Kazuhiro Sawa, Tatsuo Oku and Tadashi Maruyama, “Draft of Standard for Graphite Core Components in High Temperature Gas-cooled Reactors,” Japan Atomic Energy Agency Research 2009-042, Jan 2010.
10) James Sterbentz, “Fast Fluence to DPA Conversion Factors for the AGR Experiments in ATR,” Personal Email, Oct 19, 2019.
11) William Windes. Data Report on Post-Irradiation Dimensional Change of AGC-1 Samples. United States: N. p., 2012., Appendix A, Web. doi:10.2172/1056006.
12) J. Kestin, K. Knierim, E. A. Mason, B. Najafi, S. T. Ro, M. Waldman, “Equilibrium and Transport Properties of the Noble Gases and Their Mixtures at Low Density,” J. Phys. Chem, Vol. 13, No. 1, pp 229-303, 1984.
13) The MCNP Code Development Team, MCNP Code Manual, https://mcnp.lanl.gov/references.shtml, Los Alamos National Laboratory, accessed Dec 2017.